

University of Vermont

**UVM ScholarWorks**

---

College of Arts and Sciences Faculty  
Publications

College of Arts and Sciences

---

2-1-2019

## Human and natural controls on erosion in the Lower Jinsha River, China

Amanda H. Schmidt  
*Oberlin College*

Alison R. Denn  
*University of Vermont*

Alan J. Hidy  
*Lawrence Livermore National Laboratory*

Paul R. Bierman  
*University of Vermont*

Ya Tang  
*Sichuan University*

Follow this and additional works at: <https://scholarworks.uvm.edu/casfac>



Part of the [Climate Commons](#)

---

### Recommended Citation

Schmidt, A., Denn, A., Hidy, A., Bierman, P., & Tang, Y. (2019). Human and natural controls on erosion in the Lower Jinsha River, China. *Journal of Asian Earth Sciences*, 170(C), 351-359.

This Article is brought to you for free and open access by the College of Arts and Sciences at UVM ScholarWorks. It has been accepted for inclusion in College of Arts and Sciences Faculty Publications by an authorized administrator of UVM ScholarWorks. For more information, please contact [scholarworks@uvm.edu](mailto:scholarworks@uvm.edu).



LAWRENCE  
LIVERMORE  
NATIONAL  
LABORATORY

# Human and natural controls on erosion in the Lower Jinsha River, China

A. H. Schmidt, A. R. Denn, A. J. Hidy, P. R. Bierman, Y. Tang

May 8, 2018

Journal of Asian Earth Sciences

## **Disclaimer**

---

This document was prepared as an account of work sponsored by an agency of the United States government. Neither the United States government nor Lawrence Livermore National Security, LLC, nor any of their employees makes any warranty, expressed or implied, or assumes any legal liability or responsibility for the accuracy, completeness, or usefulness of any information, apparatus, product, or process disclosed, or represents that its use would not infringe privately owned rights. Reference herein to any specific commercial product, process, or service by trade name, trademark, manufacturer, or otherwise does not necessarily constitute or imply its endorsement, recommendation, or favoring by the United States government or Lawrence Livermore National Security, LLC. The views and opinions of authors expressed herein do not necessarily state or reflect those of the United States government or Lawrence Livermore National Security, LLC, and shall not be used for advertising or product endorsement purposes.

*For submission to the Journal of Asian Earth Sciences*

26 September 2018

Human and natural controls on erosion in the Lower Jinsha River, China

Amanda H. Schmidt<sup>1\*</sup>, Alison R. Denn<sup>2</sup>, Alan J. Hidy<sup>3</sup>, Paul R. Bierman<sup>2</sup>, Ya Tang<sup>4</sup>

1: Geology Department, Oberlin College, Oberlin, OH 44074

2: Department of Geology, University of Vermont, Burlington, VT 05405

3: Center for Accelerator Mass Spectrometry, Lawrence Livermore National Laboratory,  
Livermore, CA 94550

4: Department of Environment, Sichuan University, Chengdu, China

\* Corresponding author: [aschmidt@oberlin.edu](mailto:aschmidt@oberlin.edu)

## Abstract

1           The lower Jinsha River has the highest sediment yield rates of the entire Yangtze  
2 watershed; these high yields have previously been attributed to a mix of the local geologic  
3 setting as well as intensive human land use, particularly agriculture. Prior studies have not  
4 quantified long-term background rates of sediment generation, making it difficult to know if  
5 modern sediment yield is elevated relative to the long-term rate of sediment generation.

6           Using *in situ*  $^{10}\text{Be}$  in detrital river sediments, we measured sediment generation rates for  
7 tributaries to the lower Jinsha River. We find that the ratio of modern sediment yield to long-  
8 term sediment generation rate is  $5.9 \pm 2.8$  (mean, 1 SD,  $n = 5$ ), which is significantly higher than  
9 that elsewhere in western China and implies contemporary rates of sediment export far exceed  
10 long-term rates of sediment generation by weathering on hillslopes ( $1.9 \pm 0.9$  [median, 1 SD,  $n =$   
11 20]; (Schmidt et al., 2017)). Long-term (thousand year) rates of sediment generation correlate  
12 best with the steepness of the upstream watershed, a result found around the world. In contrast,  
13 modern sediment yield and the ratio of sediment yield to sediment generation rates correlate best  
14 with agricultural land use and distance to the nearest dam. Modern (1950s-1980s) sediment yield  
15 and the ratio of sediment yield to sediment generation also correlate well with percent of the  
16 watershed containing landslides observable today. The significantly higher modern sediment  
17 yield, lack of correlation between percent of the basin with landslides and long-term rates of  
18 sediment generation, and widespread deforestation and agriculture in the region suggest that  
19 landslide scars observable today are at least in part a result of human-induced land use change.  
20 Thus, we conclude that a mix of geologic setting and human activity control high contemporary  
21 sediment yield rates in the region.

22 **Keywords:**  $^{10}\text{Be}$ , landslides, erosion, Yangtze River, sediment yield

23

24 **Highlights**

- 25 • Long-term sediment generation rates scale with mean basin slope throughout the lower Jinsha  
26 River
- 27 • The ratio of contemporary sediment yield to long-term sediment generation is average of five  
28 • People are raising sediment yield with agriculture and deforestation and lowering it with dams  
29 • Percent of basins with landslides is positively correlated to modern sediment yield

30

## 31 **1. Introduction**

32 Human activity in the environment can change the movement of sediment across the  
33 landscape in varying ways, depending on the scale of the disturbance, size of the watershed, and  
34 type of disturbance (Syvitski et al., 2005). For example, widespread construction of dams can  
35 greatly reduce the load of sediment in rivers and agriculture and deforestation can increase  
36 erosion on hillslopes and often increases sediment yield in rivers (Hewawasam et al., 2003). In  
37 areas with high natural erosion rates, large volumetric contributions of landslides to the long-  
38 term sediment budget, and tectonically active geologic settings, it can be difficult to discern the  
39 relative increase in erosion caused by human activity (National Research Council, 2010).  
40 Landslide frequency and distribution can also be strongly influenced by human activity,  
41 including deforestation and road building (Benda and Dunne, 1997; Bierman et al., 2005).  
42 Without both long-term rates of sediment generation (often calculated using *in situ*  $^{10}\text{Be}$  in  
43 detrital river sediment (Bierman and Steig, 1996; Brown et al., 1995; Granger et al., 1996)) and  
44 modern sediment yields (from river gauging stations records in the region), it is difficult to  
45 compare short-term sediment yields influenced by human action to long-term sediment  
46 generation rates controlled by geologic factors (e.g., Kirchner et al., 2001).

47 In western China, prior studies find that human activity, in particular agricultural land use,  
48 has increased sediment yield relative to long-term rates of sediment generation by approximately  
49 a factor of two (Schmidt et al., 2017). The lower Jinsha River, east of the regions previously  
50 studied in China (Chappell et al., 2006; Schmidt et al., 2017; Schmidt et al., 2011), has long been  
51 identified as a region with unusually high contemporary rates of erosion and sediment yield  
52 (Jiang et al., 2015; Lu, 2005). These elevated erosion and sediment yield rates are typically



53 blamed on the effects of land use by humans (Jiang et al., 2015; Lu, 2005). However, prior  
54 research only considers short-term sediment yield and erosion data rather than considering long-  
55 term background rates of sediment generation as a baseline by which to evaluate the  
56 contemporary data. In this paper, we consider the dual effects of geologic setting and human  
57 activity in setting the ratio of modern sediment yield to long-term rates of sediment generation in  
58 the lower Jinsha River region of the Yangtze River watershed.

## 59 **2. Background**

60 *In situ*-produced  $^{10}\text{Be}$  ( $^{10}\text{Be}_i$ ), measured in fluvial sediment, has been used extensively to  
61 quantify rates of erosion and infer background rates of sediment generation mostly, but not  
62 exclusively, in small, headwater basins.  $^{10}\text{Be}_i$  concentration in detrital sediment is inversely  
63 related to erosion rate (Bierman and Steig, 1996; Brown et al., 1995; Granger et al., 1996) and  
64 erosion and sediment generation rates calculated from measured  $^{10}\text{Be}_i$  concentration are  
65 insensitive to human activities if depth of erosion is shallower than the mixed soil layer (~100  
66 cm) (Bierman and Steig, 1996; Brown et al., 1995; Brown et al., 1988; Granger et al., 1996;  
67 Reusser et al., 2015; Schmidt et al., 2016; Vanacker et al., 2007; Von Blanckenburg et al., 2004).

68 Many prior studies compare modern sediment yield with long-term sediment generation  
69 rates to understand if and how people are altering erosion and sediment supply to rivers (e.g.,  
70 Covault et al., 2013; Kirchner et al., 2001). When modern sediment yield and long-term  
71 sediment generation are similar (e.g., ratio ~ 1), the landscape is interpreted as being in mass  
72 steady state (Matmon et al., 2003; Wittmann et al., 2011). When modern sediment yield is  
73 significantly higher than long-term rates of sediment generation (ratio > 1), land use changes are  
74 blamed for increasing contemporary sediment yield (Hewawasam et al., 2003; Reusser et al.,

75 2015; Schmidt et al., 2017); this effect is more commonly seen in smaller watersheds  
76 (Vanmaercke et al., 2015). If long-term rates of sediment generation significantly exceed modern  
77 sediment yield (ratio < 1), then the data are interpreted as dams reducing modern sediment yield  
78 (Syvitski et al., 2005), rare but important sediment transport events being missing by short  
79 contemporary records (Kirchner et al., 2001; Tomkins et al., 2007), and dams raising apparent  
80  $^{10}\text{Be}_i$ -derived sediment generation rates through selective sourcing of sediment from below the  
81 dam (Reusser et al., 2017).

82         Prior work in China has focused on major Yangtze tributaries (Chappell et al., 2006) and  
83 western Sichuan/eastern Tibet (Schmidt et al., 2017; Schmidt et al., 2011). The Yangtze  
84 tributaries have ratios of contemporary sediment yield to long-term rates of sediment generation  
85 from 0.2 to 2.3 (mean =  $0.8 \pm 0.5$ , n = 6) (Chappell et al., 2006) and a study of the main stem of  
86 the Yangtze, Mekong, and Tsang Po rivers finds that only the Yangtze River has a ratio greater  
87 than one (1.26), while the Mekong and Tsang Po rivers have ratios of 0.57 and 0.20, respectively  
88 (Schmidt et al., 2011). The low ratios for the Mekong and Tsang Po are attributed to stochastic  
89 events such as landslides driving the long-term patterns of sediment generation but not being  
90 captured in the short-term sediment yield data (Schmidt et al., 2017). In contrast, in a large study  
91 of 20 gauging stations in Yunnan and eastern Tibet, the mean ratio of sediment yield to sediment  
92 generation is  $1.9 \pm 1.7$  (Schmidt et al., 2017). The doubling of sediment yield compared to  
93 sediment generation is attributed to human agricultural land use (Schmidt et al., 2017).

### 94 **3. Study area**

95         The lower Jinsha River is the region of the Yangtze River upstream of the confluence  
96 with the Min River and downstream of the confluence with the Yalong River (Figure 1); the river

97 forms the divide between Sichuan (to the north/west) and Yunnan (to the south/east) in this  
98 region. The study area is upstream of the Sichuan basin and appears to have a knickpoint moving  
99 through the system (Figure 2, 3), possibly due to the formation of the Sichuan basin. In the  
100 uppermost basins of the study area, the topography is rolling and the Jinsha flows through a wide  
101 open valley. In the middle of the study area, the Jinsha is incised into a deep gorge inset into  
102 rolling topography. In the downstream reaches of the study area, the landscape is steep and  
103 deeply dissected.

104 A series of four dams are being built along the main stem of the lower Jinsha River,  
105 which will collectively store 41.3 billion cubic meters of water and generate nearly double the  
106 electricity produced by the Three Gorges Dam (38 GW compared to 18.2 GW) (Yao et al., 2006).  
107 At the time of sampling, the lower two dams had been closed (Xiangjiaba and Xiluodu) while the  
108 upper dams (Wudongde and Baihetan) were still under construction. Numerous small dams,  
109 which likely trap sediment, dating back to the 1950s are present in most tributary valleys (Lu,  
110 2005).

111 Agriculture in the region is concentrated on less steep slopes, so there is an inverse  
112 correlation between agricultural land use and steepness ( $R^2 = 0.50$ ,  $p < 0.05$ ) (Figure 1). Up to 42%  
113 of the basins sampled are agricultural in land use (mean = 30%, minimum = 13%). The  
114 remaining area is a mix of primarily forest and grassland (basins are up to 72% forested [ mean =  
115 43%, minimum = 13%] and up to 50% grassland [mean = 25%, minimum = 8%]), although there  
116 are some significant lakes (one is nearly 3% of the area of one large basin; other basins are <0.5%  
117 water), urban areas (including Kunming, which accounts for >3% of one basin area; other basins  
118 are up to ~1% urban [mean = 0.6%]), and shrublands (up to nearly 5% [mean = 1.4%, minimum  
119 = 0.07%]). Although commercial logging is now banned in western China and agricultural land

120 on sloping hillslopes is being reforested, this has only happened in the last ~20 years and prior to  
121 the late 1990s; both logging and cultivation of steep land were common in western Sichuan (Trac  
122 et al., 2007; 2013; Urgenson et al., 2010).

123         Rainfall varies little over the study area. Basins average 777 to 996 mm/yr of  
124 precipitation with rainfall rates typically higher to the north of the river (in Sichuan) than to the  
125 south (in Yunnan) (Yatagai et al., 2012). The climate is monsoonal and the vast majority of the  
126 rain falls in the summer months (June, July, August, and September) (Yatagai et al., 2012). Mean  
127 annual temperature in the study region is 15°C, with maximum temperatures during the rainy  
128 season (mean = 20° C during this time) (Jiang et al., 2015). With the exception of one watershed  
129 (JS09), the region is classified as temperate, dry winter, and either hot or warm summer. JS09 is  
130 classified as Arid steppe hot (Peel et al., 2007).

131         One subcatchment we sampled, the Xiao River, is the site of the Dongchuan Debris Flow  
132 Observatory, a field site for the Chinese Academy of Sciences State Key Lab for Mountain  
133 Hazards Research (Zhou et al., 2016). This tributary to the Jinsha is considered to be the most  
134 debris flow prone region in China due to a mix of local geology – a river flowing along fractured  
135 rock in a tectonically active area – and human activity, including both mining and agriculture  
136 (Wu et al., 2016).

137         Prior work in the region focused on modern rates of sediment yield and erosion. The  
138 region is one of the highest sediment-producing areas of the Yangtze basin (Lu and Higgitt, 1998,  
139 1999). Typical narratives assert that the mix of geologic setting and human activity (agriculture)  
140 have caused the high rates of sediment yield (Jiang et al., 2015; Lu, 2005; Lu and Higgitt, 1998,  
141 1999). One modeling study finds that highest rates of erosion are on agricultural slopes between

142 15° and 35°. Modelled erosion rates range from 500 to 15,000 tons/km<sup>2</sup>-year; the mean in the  
143 study region is 5210 tons/km<sup>2</sup>-year (Jiang et al., 2015). Focusing on just one tributary of the  
144 study area (the Longchuan River, the farthest west that we sampled), a study of discharge and  
145 sediment yield reports that although soil erosion is severe in the watershed, sediment yield from  
146 the watershed is <1000 tons/km<sup>2</sup>-year because of widespread construction of reservoirs in  
147 tributary valleys since the 1950s (Lu, 2005). However, they do find a significant increase in  
148 sediment yield in the lower reaches of the watershed, which they attribute to human activity (Lu,  
149 2005). In addition, prior analysis finds that sediment yield has generally increased in agricultural  
150 areas and decreased in urban areas over the period record for gauging station data (Lu and  
151 Higgitt, 1998, 1999).

## 152 **4. Methods**

### 153 *4.1 Field methods*

154 During January 2016, we collected medium sand (250-850 µm) samples from the active  
155 river channels of nine tributaries to the lower Jinsha River (Figure 1; Table S1); five are at or  
156 near gauging stations with previously recorded sediment yield data (Lu and Higgitt, 1998, 1999).  
157 Sites were pre-selected for watersheds that span a range of basin-average slope (15° to 25°) in  
158 order to capture the range of variability in the region. Samples were collected from alluvial rivers  
159 in landscapes with varying degrees of agricultural land use. River banks were typically not  
160 agricultural, although agriculture on hillslopes in the basins is common. Although we did not see  
161 active forestry operation, we observed few forests and many bare slopes. We also observed few  
162 reforestation sites, even though the Returning Farmland to Forest Program had already been  
163 going on for more than ten years (Trac et al., 2007; 2013; Urgenson et al., 2010). In addition,

164 hillslopes frequently had small, shallow landslides and little vegetation. Bedrock appears to be  
165 covered only with shallow regolith or at the surface in much of the study area. The main stem of  
166 the Jinsha River was being dammed with a series of large dams during the time we were doing  
167 field work. In the downstream reaches of the study area, dams were already closed and the main  
168 channel of the Jinsha was a series of large lakes. All samples were collected upstream of  
169 backwater from the dams. The results for one sample (JS11) is the error weighted average of two  
170 samples (JS10 and JS11) taken ~2 km apart from one another and processed separately.

#### 171 *4.2 Basin average parameters*

172 We determined watershed boundaries using the 30 m GDEM topographic dataset (NASA  
173 LP-DAAC, 2012) and then used the same elevation dataset to extract effective elevation  
174 (Portenga and Bierman, 2011), average basin slope, and upstream area for each watershed.  
175 Rainfall data are taken from the APHRODITE dataset (Yatagai et al., 2012). This dataset is  
176 coarser than other available datasets for rainfall in the region, but has better spatial and temporal  
177 accuracy (Andermann et al., 2011). Land use was determined from the Global Land Cover (GLC)  
178 dataset (Chen et al., 2015).

179 The study area has frequent landslides (Wu et al., 2016). To quantify the area of  
180 landslides in the watersheds as a possible control on either long-term rates of sediment  
181 generation or modern sediment yield, we visually mapped landslide scars in Google Earth and  
182 then determined the percentage of each watershed that is covered by landslide source areas. The  
183 smallest landslide mapped is 22 m<sup>2</sup>, suggesting that the limit to seeing and mapping landslides is  
184 ~20 m<sup>2</sup>.

185 Carbonate rocks are common in the study area. We determined the extent of carbonate  
186 rocks from existing geologic maps (Figure 1D) (Burchfiel and Chen, 2012) and although up to

187 57% of watersheds are underlain by carbonate likely containing little or no sand-sized quartz  
188 (Table S2), these rocks are uniformly distributed across all elevations of the basins and the  
189 effective elevation used in determining basin average erosion rates does not change when we  
190 exclude areas underlain by carbonate rocks from the calculation.

#### 191 4.3 $^{10}\text{Be}_i$ data

192 Quartz from the samples was isolated and purified through a series of acid etches using a  
193 modification of the method of Kohl and Nishiizumi (1992).  $^{10}\text{Be}_i$  was extracted from quartz  
194 following the method of Corbett et al. (2016). Each batch contained one process blank and one  
195 CRONUS N standard (Jull et al., 2015). Once the quartz was dissolved in hydrofluoric acid,  
196 aliquots were removed and analyzed by inductively coupled plasma-optical emission  
197 spectroscopy (ICP-OES) to measure  $^9\text{Be}$  content (Corbett et al., 2016; Portenga et al., 2015).

198 Isotopic ratios were measured using Accelerator Mass Spectrometry (AMS) at the Center  
199 for Accelerator Mass Spectrometry at Lawrence Livermore National Labs and normalized to the  
200 ICN 07KNSTD3110 standard with an assumed  $^{10}\text{Be}/^9\text{Be}$  ratio of  $2.85 \times 10^{-12}$  (Nishiizumi et al.,  
201 2007) (Table S1). Background correction was done using full process blanks, one of which was  
202 run with each batch of 10 samples. Samples were processed in two batches at UVM with blank  
203 measurements of  $6.20 \times 10^{-16} \pm 2.97 \times 10^{-16}$  and  $2.17 \times 10^{-15} \pm 2.29 \times 10^{-16}$ ; blank measurements are at  
204 least 30 times lower than measured ratios in samples.

205 Background sediment generation rates [tons/km<sup>2</sup>-yr] were calculated from  $^{10}\text{Be}_i$   
206 concentrations using the CRONUS Earth online erosion rate calculator version 2.3 using  
207 constants file 2.3 (<http://hess.ess.washington.edu/>) (Balco et al., 2008) (see table S3 for  
208 CRONUS input table). We calculated the effective elevation of each watershed using the

209 approach of Portenga and Bierman (2011) (Table DR2). We did not adjust calculations for  
210 watersheds with dams, but recognize that this could result in overestimating sediment generation  
211 rates for samples taken in close proximity to dams if those dams effectively restrict or cut off  
212 sediment supply from upstream – something unknowable without extensive fieldwork and details  
213 of the dam operations (Reusser et al., 2017). Erosion rates for samples taken a short distance  
214 downstream of dams which cut off sediment supply have apparently higher erosion rates because  
215 sediment is sourced from downstream of the dam, an area with a lower mean elevation than the  
216 entire watershed including the area upstream of the dam. Because  $^{10}\text{Be}_i$  production scales with  
217 elevation and erosion rates scale inversely with  $^{10}\text{Be}_i$  concentration, excluding high elevation  
218 (and thus high  $^{10}\text{Be}_i$  production) regions will lower concentration and artificially raise apparent  
219 erosion rates (Reusser et al., 2017). We used the time-invariant scaling scheme of Lal (1991) and  
220 Stone (2000) and the global production rate of  $^{10}\text{Be}_i$  of  $4.10 \pm 0.35$  atoms/g-yr (Balco et al., 2008).

## 221 **5. Results and discussion**

222 Using a combination of  $^{10}\text{Be}_i$ -derived sediment generation rates and previously published  
223 sediment yield data for the region, we explore the relative influence of agricultural land use,  
224 topography, and climate on the high sediment yield in the lower Jinsha River compared to other  
225 parts of the Yangtze River system. In this section, we consider the controls on long-term rates of  
226 sediment generation, modern sediment yield, and the ratio of sediment yield to sediment  
227 generation. We then further compare our sediment generation data to a prior study modeling  
228 hillslope erosion in the lower Jinsha River (Jiang et al., 2015). Given the small number of  
229 watersheds we sampled in this study region, formal statistical tests have little power, especially  
230 for the sediment yield values and the ratio of long-term sediment generation to short-term



231 sediment yield, where only five watersheds have data. However, qualitatively plots of such data  
232 still provide qualitative insight into the behavior of the system. Quantitative statistical data are  
233 available in the data repository (table DR5).

234 Long term, background sediment generation rates in the study region vary from 25 to 418  
235 tons/km<sup>2</sup>-yr (mean = 190±129 tons/km<sup>2</sup>-yr, n = 9), but there are no systematic patterns of  
236 through the study area (Figure 4A; table S4). These rates are slightly lower than sediment  
237 generation rates measured to the west in the Mekong, Red, and Salween drainages (Schmidt et al.,  
238 2017) and on the high end of those for other eastern tributaries to the Yangtze (Chappell et al.,  
239 2006). Long-term rates of sediment generation correlate best with the distance to the first dam  
240 upstream of the sample and the mean hillslope steepness in the watershed (Figure 4); both are  
241 positive correlations. In studies elsewhere, distance to dams is inversely correlated with erosion  
242 rates (and sediment generation rates) because dams bias sediment to come from lower altitude  
243 locations with lower <sup>10</sup>Be<sub>i</sub> production rates (Reusser et al., 2017). We interpret the positive  
244 correlation with distance to dams as an indication that both higher sediment generation rates and  
245 dams are found in steeper areas.

246 The positive correlation between the hillslope steepness in the upstream watershed and  
247 sediment generation rates suggests that steeper hillslopes typically have higher rates of sediment  
248 generation, a result that has been found in other studies using <sup>10</sup>Be<sub>i</sub> to derive sediment  
249 generation and erosion rates (as summarized in Portenga and Bierman, 2011). This could be  
250 related to the knickpoint moving through the region – high, flat, and undissected parts of the  
251 watershed are less likely to have dams and likely to have lower erosion rates, while incised and  
252 steeper parts of the watersheds are more likely to have both dams and higher erosion rates.

253 Five of the basins also have sediment yield data (1950s-1987) from Chinese gauging  
254 stations (Lu and Higgitt, 1998, 1999), which vary from 624 to 2792 tons/km<sup>2</sup>-yr (mean =  
255 1297±873 tons/km<sup>2</sup>-yr, n = 5). These data were collected during a period of expanding  
256 agriculture and deforestation throughout China (Schmidt et al., 2011). As with the long-term  
257 rates of sediment generation, sediment yield values are not systematically distributed in the study  
258 area (Figure 4b). In addition, sediment yield does not correlate significantly with any metrics we  
259 analyzed (Figure 5). This is likely due to the small number of gauging stations included within  
260 our study area and noise in the sediment yield record. The strongest correlation is with distance  
261 to the first dam, where sediment yield rates are positively correlated with distance to dam. Dams  
262 date to as early as the 1950s and sediment yield data from the 1950s-1987 (Lu and Higgitt, 1999).  
263 Dams trap sediment and thus will artificially lower sediment yields; a longer distance to dams  
264 will thus increase sediment yield from intervening hillslopes. We also see an inverse relationship  
265 between sediment yield and basin area due to increased trapping of sediment and overall lower  
266 sediment delivery ratios with increasing basin area (Trimble, 1977). Finally, we see a direct  
267 relationship between percent agriculture in the upstream watershed and sediment yield.  
268 Agriculture typically increases erosion and thus sediment yield, as has been observed elsewhere  
269 in China (Schmidt et al., 2017; 2011).

270 When considering the ratio of long-term rates of sediment generation to short-term rates  
271 of sediment yield, ratios range from 2.9 – 9.4 (mean = 5.9±2.8, n = 5); the highest ratio  
272 corresponds to the basin with the highest short-term sediment yield and second highest long-term  
273 sediment generation rate (Figure 4C). The ratio of modern rates of sediment yield to long-term  
274 rates of sediment generation does not have any significant correlations with the parameters  
275 considered, although generally the data follow the same patterns as the modern sediment yield

276 data – direct correlations with area in agriculture, distance to the nearest dam, slope, and percent  
277 of the basin with landslides and inverse correlations with basin area and mean annual  
278 precipitation (Figure 5). In terms of geologic control, we see that slope steepness is directly  
279 related to the ratio of modern sediment yield to long-term sediment generation. In terms of  
280 human effects on the system, it seems that dams are artificially lowering the modern sediment  
281 yield (e.g., Covault et al., 2013; Syvitski et al., 2005) and thus the ratio between modern  
282 sediment yield and long-term sediment generation. In contrast, agriculture appears to be  
283 generally raising the ratio of modern sediment yield to long-term sediment generation in the  
284 study area.

285         Landslides could be entirely a natural geologic control or increased by human activity  
286 (deforestation, road building, and agriculture) in the region (Benda and Dunne, 1997). If the  
287 landslides were entirely geologic in origin, we would expect the  $^{10}\text{Be}_i$ -derived sediment  
288 generation rates to account for these slides because the basins are large enough to integrate the  
289 sediment from landslides (Niemi et al., 2005). However, we find a significantly higher modern  
290 sediment yield compared to long-term sediment generation. In addition, although the region is  
291 classified as a humid temperate climate, there are few trees in the study area. Thus, it appears  
292 that landslides in this region are in large part caused by current and/or previous deforestation and  
293 agriculture and the effect of landslides in raising sediment yield is a human rather than geologic  
294 factor. Thus, we conclude that the ratio of modern sediment yield to long-term sediment  
295 generation is driven primarily by human factors.

296         We find that previously modeled RUSLE erosion rates (Jiang et al., 2015) correlate to our  
297 new long-term sediment generation rates ( $R^2 = 0.51$ ,  $p < 0.05$ ), but the mean of modelled rates is  
298 28 times higher (17-166 times). Similarly, the RUSLE-derived erosion rates are a mean of five

299 times (1.9 to 6.3 times) greater than sediment yield values in the region. Since land use,  
300 topography, and precipitation are inputs into the RUSLE model, it is not possible to further  
301 explore parameters controlling this ratio – they would be auto-correlated. However, these data  
302 suggest that modern hillslope erosion is several times higher than modern sediment yield which  
303 is, in turn, several times higher than sediment generation rates.

304 The high rates of modern erosion and sediment yield relative to long-term rates of  
305 sediment generation suggest unsustainable erosion in the study area, as previously found in the  
306 eastern United States (Reusser et al., 2017). The sediment being eroded off the hillslopes must be  
307 accumulating somewhere in the watersheds because it is not all making it to the rivers (Trimble,  
308 1977). It seems likely that the sediment is accumulating in reservoirs as well as in terraces,  
309 alluvial fans, and toe slope deposits throughout the watershed, a hypothesis confirmed by  
310 observations of sediment choked channels and alluvial fans observed in the field (Figure 6).

## 311 **6. Conclusions**

312 Using long-term rates of sediment generation from nine tributaries to the lower Jinsha  
313 River and sediment yield data from five gauging stations with data from the 1950s-1987 located  
314 near those tributaries, we find that the ratio of modern sediment yield to long-term sediment  
315 generation is controlled by a mix of agriculture, dams, and landslides in the watersheds.  
316 Agricultural activity does not seem to play as large a role in setting those ratios as dams and  
317 landslides despite known increase in local erosion due to agriculture. At the basin scale and on  
318 short time scales, human activity decreases sediment yield in rivers through dam construction.  
319 Slope steepness appears to control long-term rates of sediment generation while the frequency of

320 landslides, which at least in part are due to human activity in the watershed, controls both the  
321 ratio of long-term to modern and the modern sediment yield.

## 322 **Acknowledgements**

323 The authors would like to thank S. Doak, M. Hill, M. Byerly, L. Leslie, and Y. Wang for  
324 assistance in the field. X. Lu provided the modern sediment yield data. The work was funded by  
325 an Oberlin College Grant in Aid award to A. H. Schmidt, an Oberlin College Powers Travel  
326 Grant to A. H. Schmidt, a National Science Foundation Award to P. R. Bierman (NSF-EAR-  
327 1114159), and the Program of Introducing Talents of Discipline to Universities or “111 Project”  
328 of China award to Y. Tang (B08037). This work was performed under the auspices of the U.S.  
329 Department of Energy by Lawrence Livermore National Laboratory under Contract DE-AC52-  
330 07NA27344. This is LLNL-JRNL-751018.

331

- 334 Andermann, C., Bonnet, S., and Gloaguen, R., 2011, Evaluation of precipitation data sets along the  
335 Himalayan front: *Geochemistry, Geophysics, Geosystems*, v. 12, no. 7, p. Q07023.
- 336 Balco, G., Stone, J. O., Lifton, N. A., and Dunai, T. J., 2008, A complete and easily accessible means of  
337 calculating surface exposure ages or erosion rates from  $^{10}\text{Be}$  and  $^{26}\text{Al}$  measurements: *Quaternary*  
338 *Geochronology*, v. 3, p. 174-195.
- 339 Benda, L., and Dunne, T., 1997, Stochastic forcing of sediment supply to channel networks from  
340 landsliding and debris flow: *Water Resources Research*, v. 33, no. 12, p. 2849-2863.
- 341 Bierman, P. R., Howe, J., Stanley-Mann, E., Peabody, M., Hilke, J., and Massey, C. A., 2005, Old images  
342 record landscape change through time: *GSA Today*, v. 15, no. 4, p. 4-10.
- 343 Bierman, P. R., and Steig, E. J., 1996, Estimating rates of denudation using cosmogenic isotope  
344 abundances in sediment: *Earth Surface Processes and Landforms*, v. 21, p. 125-139.
- 345 Brown, E. T., Stallard, R. F., Larsen, M. C., Raisbeck, G. M., and Yiou, F., 1995, Denudation rates  
346 determined from the accumulation of in-situ produced  $^{10}\text{Be}$  in the Luquillo Experimental Forest,  
347 Puerto Rico: *Earth and Planetary Science Letters*, v. 129, p. 193-202.
- 348 Brown, L., Pavich, M. J., Hickman, R. E., Klein, J., and Middleton, R., 1988, Erosion of the Eastern  
349 United States observed with  $^{10}\text{Be}$ : *Earth Surface Processes and Landforms*, v. 13, p. 441-457.
- 350 Burchfiel, B. C., and Chen, Z., 2012, *Tectonics of the Southeastern Tibetan Plateau and its adjacent*  
351 *foreland (Vol. 210)*, Boulder, CO, The Geological Society of America.
- 352 Chappell, J., Zheng, H. B., and Fifield, K., 2006, Yangtse River sediments and erosion rates from source  
353 to sink traced with cosmogenic Be-10: *Sediments from major rivers: Palaeogeography*  
354 *Palaeoclimatology Palaeoecology*, v. 241, no. 1, p. 79-94.
- 355 Chen, J., Chen, J., Liao, A., Cao, X., Chen, L., He, C., Han, G., Peng, S., Lu, M., Zhang, W., Tong, X.,  
356 and Mills, J., 2015, Global land cover mapping at 30 m resolution: A POK-based operational  
357 approach: *ISPRS Journal of Photogrammetry and Remote Sensing*, v. 103, p. 7-27.
- 358 Corbett, L. B., Bierman, P. R., and Rood, D. H., 2016, An approach for optimizing *in situ* cosmogenic  
359  $^{10}\text{Be}$  sample preparation: *Quaternary Geochronology*, v. 33, p. 24-34.
- 360 Covault, J. A., Craddock, W. H., Romans, B. W., Fildani, A., and Gosai, M., 2013, Spatial and temporal  
361 variations in landscape evolution: Historic and longer-term sediment flux through global  
362 catchments: *Journal of Geology*, v. 121, no. 1, p. 35-56.
- 363 Granger, D. E., Kirchner, J. W., and Finkel, R. C., 1996, Spatially averaged long-term erosion rates  
364 measured from in-situ produced cosmogenic nuclides in alluvial sediment: *The Journal of*  
365 *Geology*, v. 104, p. 249-257.
- 366 Hewawasam, T., Von Blanckenburg, F., Schaller, M., and Kubik, P. W., 2003, Increase of human over  
367 natural erosion rates in tropical highlands constrained by cosmogenic nuclides: *Geology*, v. 33, no.  
368 7, p. 597-600.
- 369 Jiang, L., Yao, Z., Liu, Z., Wu, S., Wang, R., and Wang, L., 2015, Estimation of soil erosion in some  
370 sections of Lower Jinsha River based on RUSLE: *Natural Hazards*, v. 76, no. 3, p. 1831-1847.
- 371 Jull, A. J. T., Scott, E. M., and Bierman, P., 2015, The CRONUS-Earth inter-comparison for cosmogenic  
372 isotope analysis: *Quaternary Geochronology*, v. 26, p. 3-10.
- 373 Kirchner, J. W., Finkel, R. C., Riebe, C. S., Granger, D. E., Clayton, J. L., King, J. G., and Megahan, W.  
374 F., 2001, Mountain erosion over 10 yr, 10 k.y., and 10 m.y. time scales: *Geology* v. 29, no. 7, p.  
375 591-594.
- 376 Kohl, C. P., and Nishiizumi, K., 1992, Chemical isolation of quartz for measurement of in-situ produced  
377 cosmogenic nuclides: *Geochimica et Cosmochimica Acta*, v. 56, p. 3583-3587.
- 378 Lal, D., 1991, Cosmic ray labeling of erosion surfaces: *in situ* nuclide production rates and erosion  
379 models: *Earth and Planetary Science Letters*, v. 104, p. 424-439.

380 Lu, X., 2005, Spatial variability and temporal change of water discharge and sediment flux in the lower  
381 Jinsha tributary: impact of environmental changes: *River Research and Applications*, v. 21, no. 2  
382 - 3, p. 229-243.

383 Lu, X. X., and Higgitt, D. L., 1998, Recent changes of sediment yield in the Upper Yangtze, China:  
384 *Environmental Management*, v. 22, no. 5, p. 697-709.

385 -, 1999, Sediment yield variability in the Upper Yangtze, China: *Earth Surface Processes and Landforms*,  
386 v. 24, no. 12, p. 1077-1093.

387 Matmon, A., Bierman, P. R., Larsen, J., Southworth, S., Pavich, M. J., Finkel, R. C., and Caffee, M. W.,  
388 2003, Erosion of an ancient mountain range, the Great Smoky Mountains, North Carolina and  
389 Tennessee: *American Journal of Science*, v. 303, p. 517-855.

390 NASA LP-DAAC, 2012, ASTER GDEM, *in* NASA Land Processes Distributed Active Archive Center  
391 (LP DAAC), ed., LP DAAC.

392 National Research Council, 2010, *Landscapes on the edge: New horizons for research on Earth's surface*,  
393 national academies Press.

394 Niemi, N. A., Oskin, M., Burbank, D. W., Heimsath, A. M., and Gabet, E. J., 2005, Effects of bedrock  
395 landslides on cosmogenically determined erosion rates: *Earth and Planetary Science Letters*, v.  
396 237, p. 480-498.

397 Nishiizumi, K., Imamura, M., Caffee, M. W., Southon, J. R., Finkel, R. C., and McAninch, J., 2007,  
398 Absolute calibration of  $^{10}\text{Be}$  AMS standards: *Nuclear Instruments and Methods B*, v. 258, no. 2, p.  
399 403-413.

400 Peel, M. C., Finlayson, B. L., and McMahon, T. A., 2007, Updated world map of the Koppen-Geiger  
401 climate classification: *Hydrology and Earth System Sciences*, v. 11, no. 5, p. 1633-1644.

402 Portenga, E. W., and Bierman, P. R., 2011, Understanding Earth's eroding surface with  $^{10}\text{Be}$ : *GSA Today*,  
403 v. 21, no. 8, p. 4-10.

404 Portenga, E. W., Bierman, P. R., Duncan, C., Corbett, L. B., Kehrwald, N. M., and Rood, D. H., 2015,  
405 Erosion rate of the Bhutanese Himalaya determined using *in situ*-produced  $^{10}\text{Be}$ : *Geomorphology*,  
406 v. 233, p. 112-126.

407 Reusser, L. J., Bierman, P. R., Rizzo, D. M., Portenga, E. W., and Rood, D. H., 2017, Characterizing  
408 landscape-scale erosion using  $^{10}\text{Be}$  in detrital fluvial sediment: Slope-based sampling strategy  
409 detects the effect of widespread dams: *Water Resources Research*, v. 53.

410 Reusser, L. J., Bierman, P. R., and Rood, D. H., 2015, Quantifying human impacts on rates of erosion and  
411 sediment transport at a landscape scale: *Geology* v. 43, no. 2, p. 171-174.

412 Schmidt, A. H., Gonzalez, V. S., Bierman, P. R., Neilson, T. B., and Rood, D. H., 2017, Agricultural land  
413 use doubled sediment loads in western China's rivers: *Anthropocene*.

414 Schmidt, A. H., Montgomery, D. R., Huntington, K. W., and Liang, C., 2011, The question of communist  
415 land degradation: New evidence from local erosion and basin-wide sediment yield in Southwest  
416 China and Southeast Tibet: *Annals of the Association of American Geographers*, v. 101, no. 3, p.  
417 1-20.

418 Schmidt, A. H., Neilson, T. B., Bierman, P. R., Rood, D. H., Ouimet, W. B., and Sosa Gonzalez, V., 2016,  
419 Influence of topography and human activity on apparent *in situ*  $^{10}\text{Be}$ -derived erosion rates in  
420 Yunnan, SW China: *Earth Surface Dynamics*, v. 4, no. 4, p. 819-830.

421 Stone, J. O., 2000, Air pressure and cosmogenic isotope production: *Journal of Geophysical Research*, v.  
422 105, no. B10, p. 23,573-523,579.

423 Syvitski, J. P. M., Vorosmarty, C. J., Kettner, A. J., and Green, P., 2005, Impact of humans on the flux of  
424 terrestrial sediment to the global coastal ocean: *Science*, v. 308, no. 5720, p. 376-380.

425 Tomkins, K., Humphreys, G., Wilkinson, M., Fink, D., Hesse, P., Doerr, S., Shakesby, R., Wallbrink, P.,  
426 and Blake, W., 2007, Contemporary versus long - term denudation along a passive plate margin:  
427 the role of extreme events: *Earth Surface Processes and Landforms*, v. 32, no. 7, p. 1013-1031.

- 428 Trac, C. J., Harrell, S., Hinckley, T. M., and Henck, A. C., 2007, Reforestation programs in Southwest  
429 China: Reported success, observed failures, and the reasons why: *Journal of Mountain Science*, v.  
430 4, no. 4, p. 275-292.
- 431 Trac, C. J., Schmidt, A. H., Harrell, S., and Hinckley, T. M., 2013, Is the returning farmland to forest  
432 program a success? Three case studies from Sichuan: *Environmental Practice*, v. 15, no. 3, p.  
433 350-366.
- 434 Trimble, S. W., 1977, Fallacy of Stream Equilibrium in Contemporary Denudation Studies: *American*  
435 *Journal of Science*, v. 277, no. 7, p. 876-887.
- 436 Urgenson, L. S., Hagemann, R. K., Henck, A. C., Harrell, S., Hinckley, T. M., Shepler, S. J., Grub, B. L.,  
437 and Chi, P. M., 2010, Social-ecological resilience of a Nuosu community-linked watershed,  
438 southwest Sichuan, China: *Ecology and Society*, v. 15, no. 4, p. 2.
- 439 Vanacker, V., Von Blanckenburg, F., Govers, G., Molina, A., Poesen, J., Deckers, J., and Kubik, P., 2007,  
440 Restoring dense vegetation can slow mountain erosion to near natural benchmark levels: *Geology*  
441 v. 35, no. 4, p. 303-306.
- 442 Vanmaercke, M., Poesen, J., Govers, G., and Verstraeten, G., 2015, Quantifying human impacts on  
443 catchment sediment yield: A continental approach: *Global and Planetary Change*, v. 130, p. 22-36.
- 444 Von Blanckenburg, F., Hewawasam, T., and Kubik, P. W., 2004, Cosmogenic nuclide evidence for low  
445 weathering and denudation in the wet, tropical highlands of Sri Lanka: *Journal of Geophysical*  
446 *Research: Earth Surface*, v. 109, no. F3, p. F03008.
- 447 Wittmann, H., von Blanckenburg, F., Maurice, L., Guyot, J. L., Filizola, N., and Kubik, P. W., 2011,  
448 Sediment production and delivery in the Amazon River basin quantified by *in situ*-produced  
449 cosmogenic nuclides and recent river loads: *Geological Society of America Bulletin*, v. 123, no.  
450 5-6, p. 934-950.
- 451 Wu, Y., Liu, X., Liu, L., and Shi, P., 2016, *Landslide and Debris Flow Disasters in China*, Natural  
452 Disasters in China, Springer, p. 73-101.
- 453 Yatagai, A., Kamiguchi, K., Arakawa, O., Hamada, A., Yasutomi, N., and Kitoh, A., 2012, APHRODITE:  
454 Constructing a long-term daily gridded precipitation dataset for Asia based on a dense network of  
455 rain gauges: *Bulleting of the American Meteorological Society*, v. 39, no. 9, p. 1401-1415.
- 456 Yao, Y.H., Zhang, B.P., Ma, X.D., and Ma, P., 2006, Large-scale hydroelectric projects and mountain  
457 development on the upper Yangtze river: *Mountain Research and Development*, v. 26, no. 2, p.  
458 109-114.
- 459 Zhou, G. G., Ouyang, C., and Chen, X., 2016, Key Laboratory of Mountain Hazards and Earth Surface  
460 Processes, Chinese Academy of Sciences: *Mountain Research and Development*, v. 36, no. 1, p.  
461 116-118.

462

463



## Figure captions

Figure 1: (A) Location of the study area in Asia. (B) Distribution of rainfall (Yatagai et al., 2012), sample sites, first dams, and basin boundaries in the study area. Italicized numbers and letters show approximate location of pictures in figures 2 and 6. (C) Slopes in the study area (NASA LP-DAAC, 2012). (D) Carbonate rocks (large orange shapes) (Burchfiel and Chen, 2012) and landslides (small purple shapes) in the study basins. (E) Land use throughout the study area and surrounding region (Chen et al., 2015).

Figure 2: Photos of the field sites going from upstream (A) to downstream (D) that show the increasing incision in the landscape due to the upstream propagation of knickpoints. (A) Photo taken at site JS09. (B) Photo taken from sample JS06 towards main stem of the Jinsha. (C) Photo taken of main stem of the Jinsha from road between samples JS03 and JS04. The cliffs seen are only a few meters tall on the main stem of the Jinsha near sample JS05. (D) Photo taken near sample JS03. Approximate location of photos shown in figure 1B.

Figure 3: Long profiles of the main stem (black) and sampled tributaries (grey) showing the location of the main stem knickpoint. Profiles are smoothed using a kernel smoothing algorithm.

Figure 4: Maps showing (A) long-term sediment generation rates, (B) modern sediment yield rates (Lu and Higgitt, 1998, 1999), and (C) the ratio of sediment yield to sediment generation.

Figure 5: Correlations between measures of erosion (from top to bottom: sediment generation rate, sediment yield rate, and the ratio of sediment yield to sediment generation) as a function of basin average parameters (from left to right: % agriculture in the basin, basin area, distance to first dam, % landslides in the upstream basin, mean slope of the basin, and mean annual precipitation). All correlations discussed are detailed in table DR5.

Figure 6: Pictures in the study area showing the vegetation, landslides, and sediment storage. (A) Large rocks, small toe slope storage, and bare hillslopes near JS07; (B) Shallow landslides, deforested hillslopes, and sediment storage near JS11; (C) In channel sediment storage near JS05; (D) Alluvial fan and sediment storage in the main stem of the Jinsha near JS05; (E) Shallow landsliding and in channel sediment storage at JS08; (F) Shallow landsliding, bare hillslopes, and in channel sediment storage near JS08. Approximate photo locations shown on figure 1B.

Figure 1  
[Click here to download high resolution image](#)

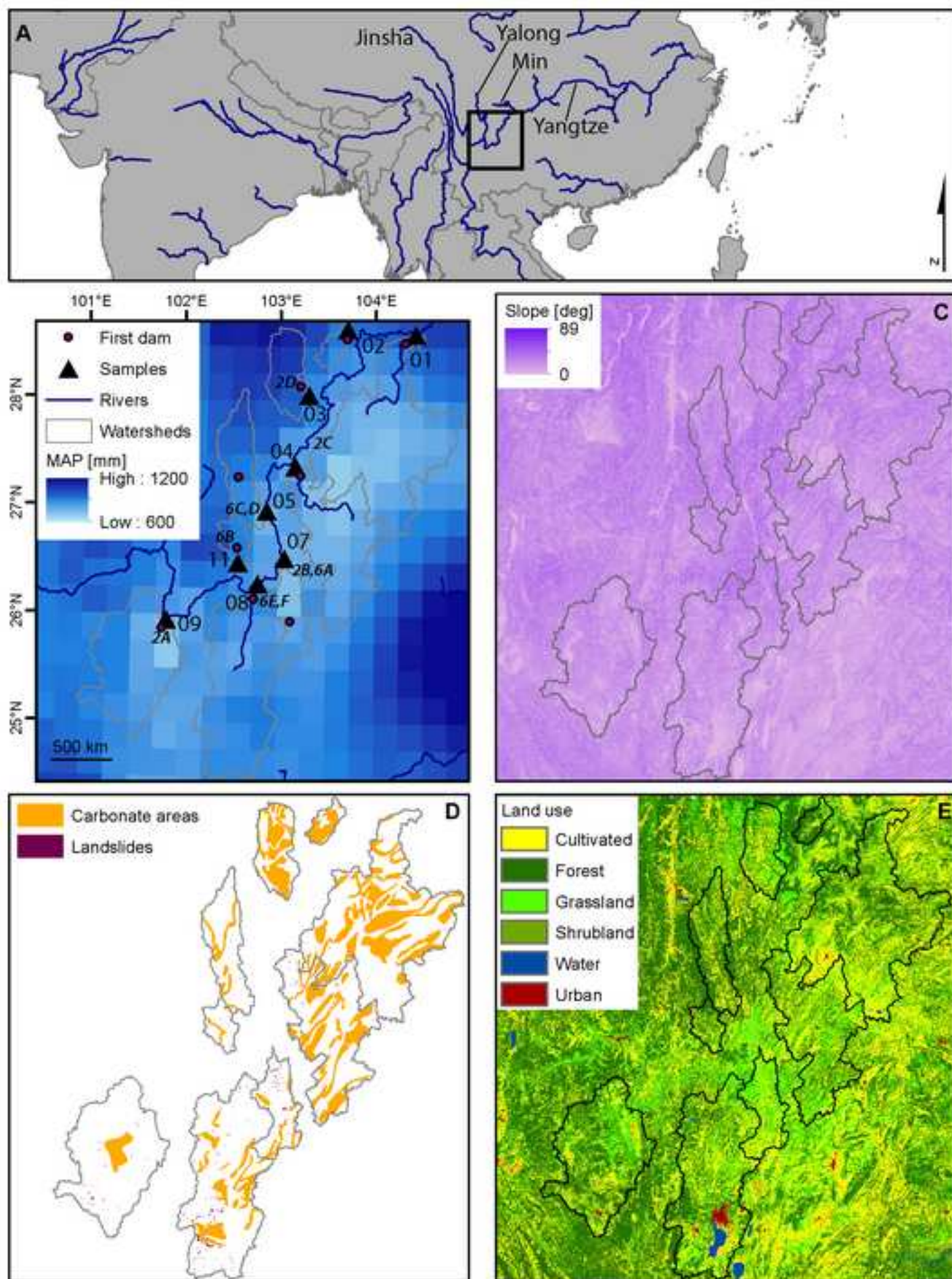
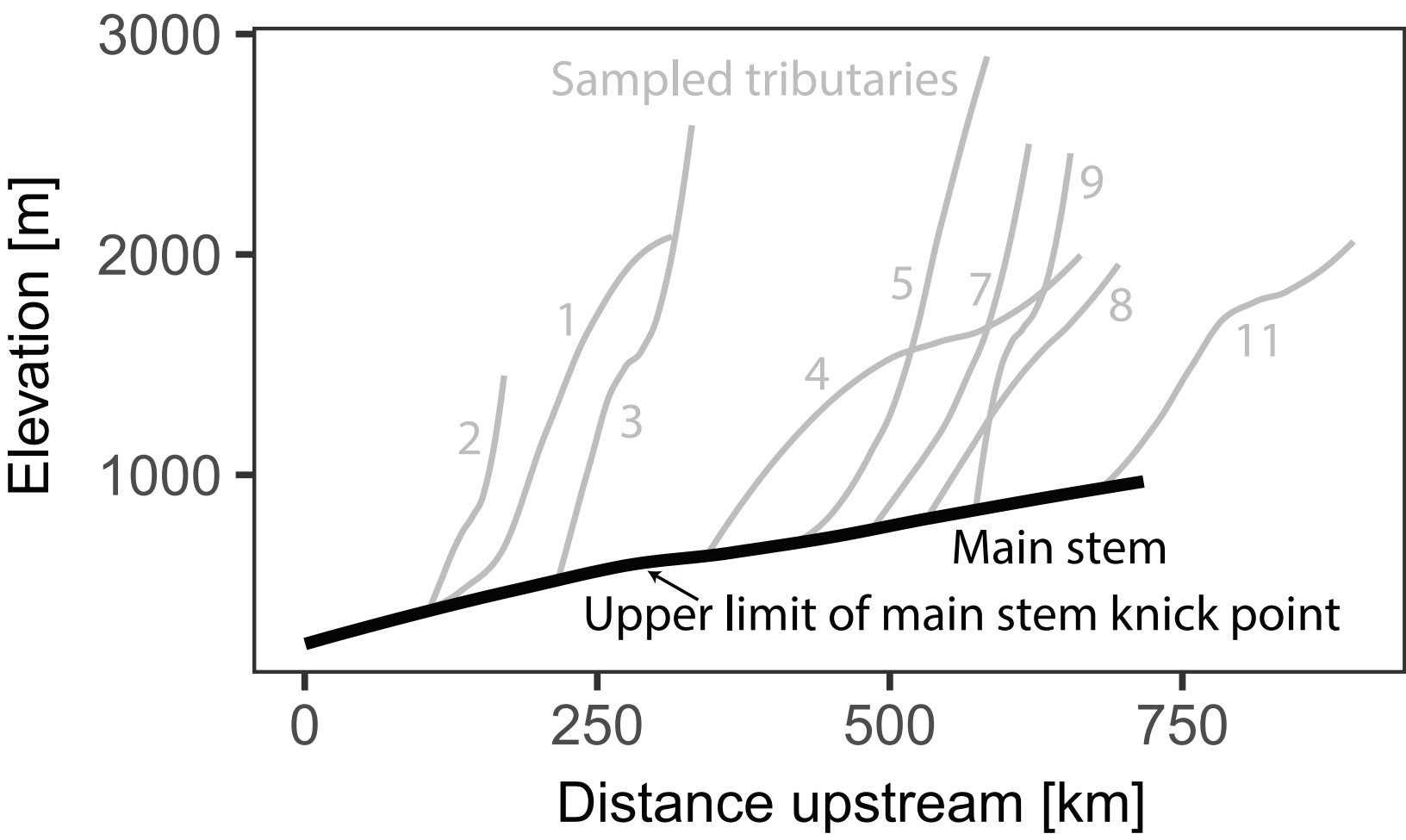


Figure 2  
[Click here to download high resolution image](#)



Figure 3



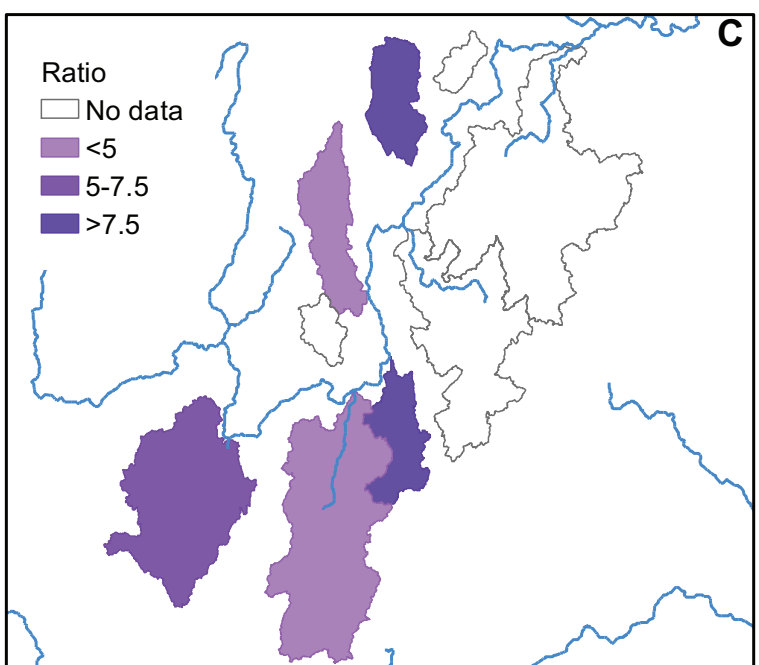
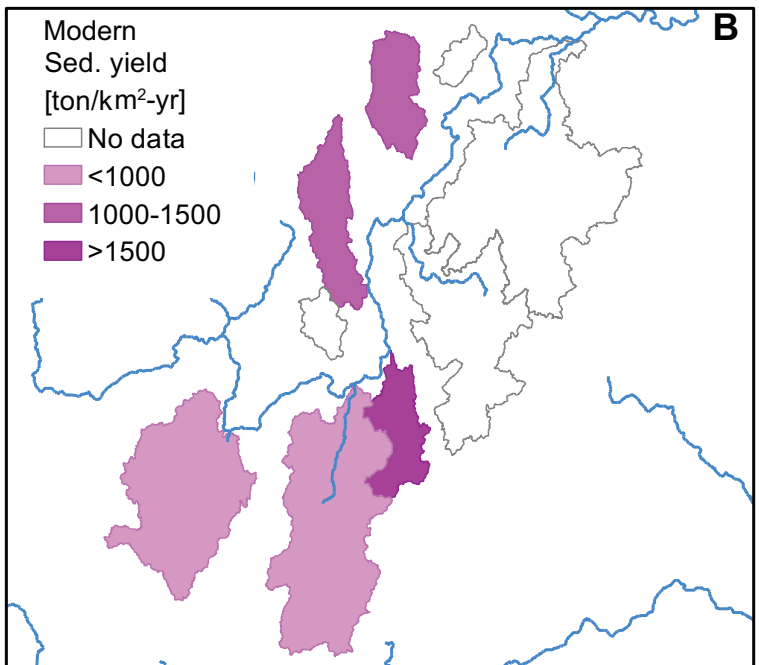
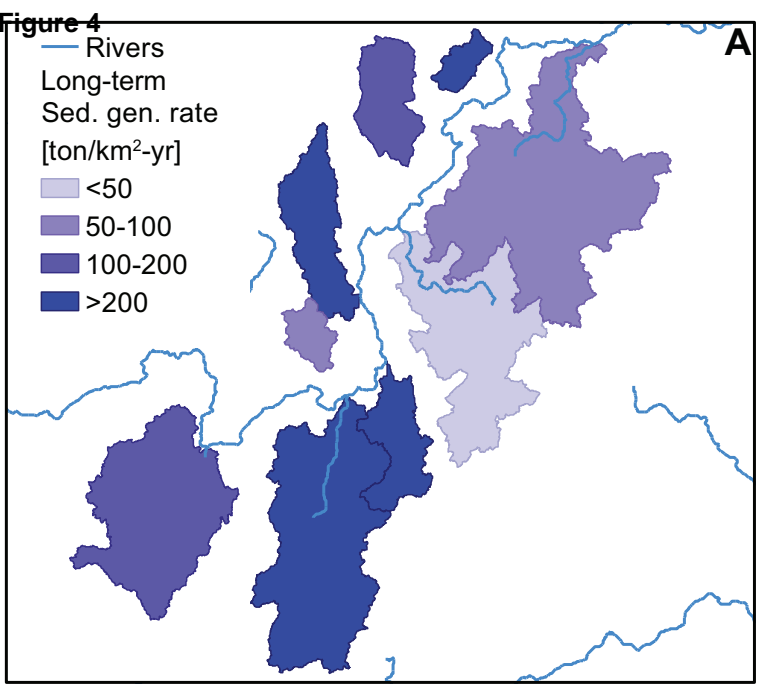
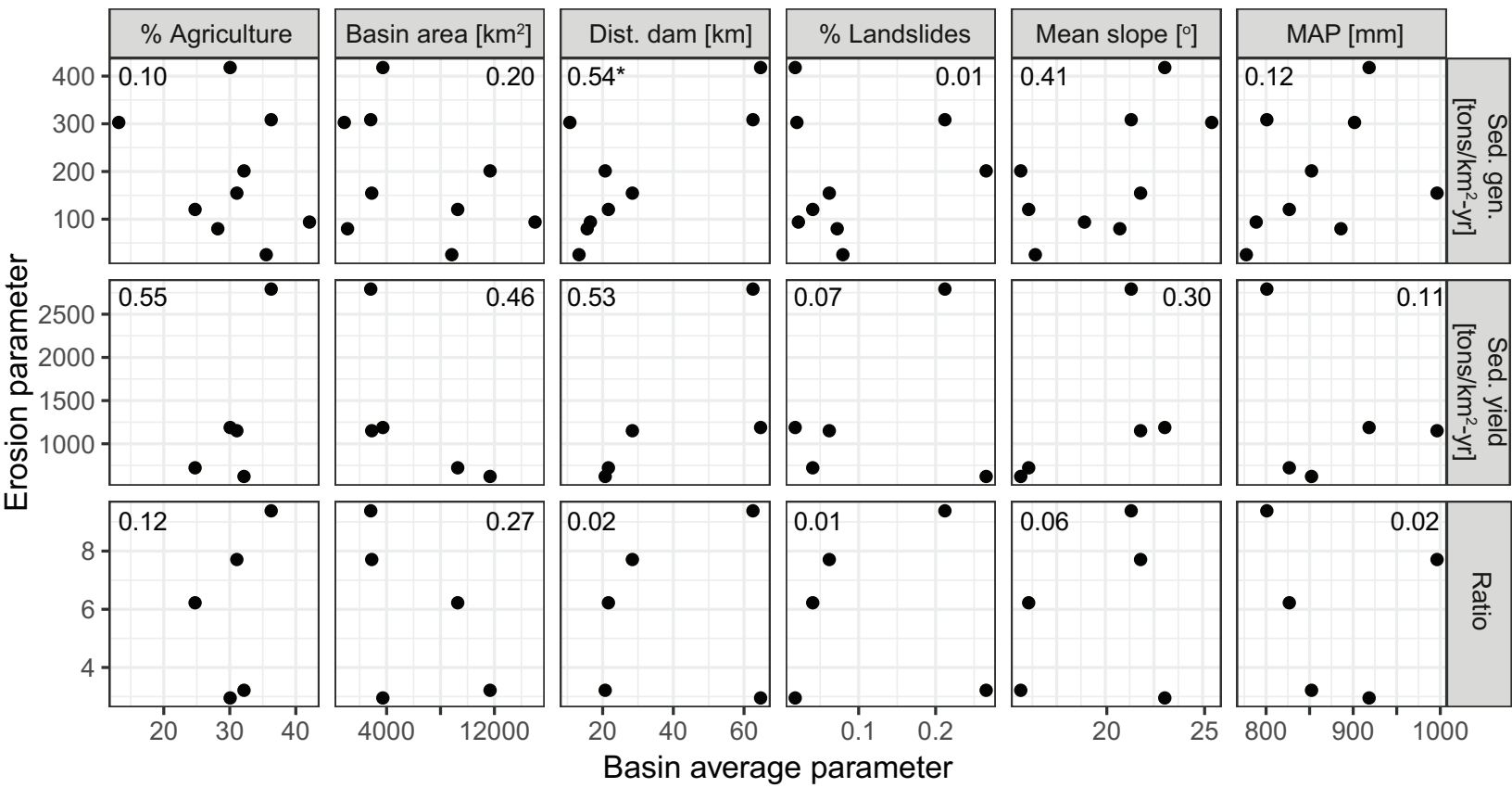


Figure 5



**Figure 6**  
[Click here to download high resolution image](#)

